DISTRIBUTED FIBER-OPTIC TEMPERATURE PROFILING ALONG FULL ESP SYSTEMS IN GASSY UNCONVENTIONAL WELLS

Araceli Rivera Mandujano and Michael Rumbaugh
SLB

Cody Casey and Scott Schulte
Diamondback

Mario Campos
Amplified Industries (Former SLB Employee)

ABSTRACT

The thermal behavior of Electrical Submersible Pump (ESP) systems deployed in unconventional wells is poorly characterized, particularly when exposed to elevated gas volume fractions and transient flow regimes. Traditional point temperature measurements provide limited spatial resolution and do not capture how gas interference influences heat distribution along pump stages, seal sections, and motors. To address this knowledge gap, an experimental R&D deployment of distributed fiber-optic temperature sensing (DTS) was performed in a gassy unconventional well to observe continuous downhole temperature profiles along the entire ESP assembly. The DTS system was encapsulated in a stainless-steel tube and installed externally along the ESP string, from the sensor to above discharge. The acquired data showed distinct temperature changes associated with gas-entrainment regions, as well as deviations in cooling performance from values typically assumed in ESP selection and modeling.
The intent of this work is not to propose a scalable field monitoring method, but to present rare empirical insight into actual ESP thermal profiles in gassy unconventional wells. The findings can help refine operating envelope interpretation, improve cooling-related design assumptions, and enhance diagnostic understanding using existing surveillance signals.

INTRODUCTION

Unconventional resource development targets tight and nearly impermeable shale and tight rock formations that contain significant hydrocarbon volumes previously inaccessible using conventional drilling techniques. Although development of these reservoirs involves higher drilling and completion costs, their economic viability depends on maximizing early productivity and minimizing time to break even. Artificial lift methods are therefore employed not only to sustain production after natural flow ceases, but also to maximize production while the wells are still flowing naturally.

Electric submersible pumps (ESPs) are widely deployed in unconventional wells due to their broad operating range and moderate efficiency. They can be installed early in the well lifecycle and remain operational through depletion or until production rates favor alternative artificial lift systems. However, ESPs represent the highest-cost artificial lift option in terms of both capital and operating expenditures, making reliability a critical performance metric.

Initial deployments of ESPs in unconventional U.S. wells demonstrated that conventional system designs were often ill-suited for these environments. Key challenges include rapid pressure and rate declines, elevated gas–liquid ratios (GLR) with slug flow behavior, high reservoir temperatures, sand production, corrosive fluids, and deep wellbores. These conditions significantly increase the likelihood of thermal and mechanical degradation.

While advancements in monitoring, materials, and surface control systems have been made, pump hydraulic designs have remained largely unchanged since their development in the early 1900s. Consequently, industry efforts have focused on improving system reliability through enhanced diagnostics, control logic, and operational mitigation strategies.

Evaluation of real-time downhole sensor data in combination with ESP teardown analyses indicates that gas related phenomena are a primary contributor to failure mechanisms in unconventional wells in the Permian Basin. Tight casing geometries limit gas venting, reducing the effectiveness of gas separation devices. Elevated temperatures are frequently observed during ESP operation, particularly within the pump section. Periods of reduced electrical current are often followed by increases in motor temperature, consistent with gas induced no-flow conditions that restrict fluid circulation and reduce motor cooling.

Variable speed drive (VSD) control algorithms represent a key mitigation mechanism by enabling real-time operational adjustments intended to alleviate gas-lock conditions and prevent repeated thermal shutdowns. Protective logic based on low current and high motor temperature thresholds can reduce the probability of thermally induced failures such as electrical damage and material degradation. However, due to the transient and highly variable nature of unconventional wells, no single control strategy consistently yields optimal results.

This high unpredictability in unconventional wells motivated this team to deploy an experimental distributed fiber-optic sensing system to measure real-time temperature profiles from surface to the kickoff point (KOP). The selected wells were completed in a formation characterized by high gas production (Wolcamp-A), which is known to present a challenge for ESPs when reaching below the bubble point.

The primary objectives of the study were to correlate surface operating parameters with downhole thermal responses, develop hypotheses regarding subsurface flow behavior,

and establish best practices for applying this methodology across different formations. Observations exceeded initial expectations: both ESP systems operated successfully from initial production through conditions below the bubble point and were only removed when the wells became better suited for alternative artificial lift methods. No ESP failures occurred, allowing for complete observation of the well's operational lifecycles.

Key observations included thermal profiles along the tubing during start-up and shutdown, pump and motor response during gas-lock events, the thermal impact of closed surface valves, and the effectiveness of modified gas-lock control logic. These results demonstrate the value of high-resolution temperature profiling in improving ESP protection strategies and enhancing system reliability in unconventional applications.

METHODOLOGY

The project was designed to install a fiber optic line from surface to the bottom of the ESP and 102 ft below the ESP sensor in two new wells to measure distributed temperatures along the ESP, with the purpose of understanding temperature behavior along ESP and under different real operating conditions.

The primary components of the DTS (Downhole Temperature Sensing) system consisted of a Downhole Fiber Optic Cable (FOC) and a Surface Interrogator. The DTS unit detects a temperature measurement every four minutes along the entire length of the cable and downhole components, which produces snapshots of the entire temperature profile from surface to the kick-off point, and those can be graphed together to see changes over time.

The FOC and ESP cable were deployed on the outside of production tubing and secured with Cross Collar Cable protectors. The FOC was terminated at the wellhead and connected to the Surface DTS Interrogator via a junction box and fiber optic surface cable. The DTS unit was housed inside a NEMA 3 rated cabinet at a suitable location close to the VSD. The interrogator was controlled and monitored remotely via cellular communications to allow changes to sample rates of the DTS and transmit data remotely.

DTS (Distributed Temperature Sensing) System

Fiber Optic Sensing Cable Specifications:

- Cable Type: Tube Encased Fiber (TEF) (Figure 1)
- Temperature rating: 200 °C (392 °F)
- Outer tube: 4mm OD; 0.028" wall; 316L

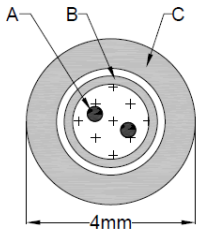

Figure 1. Fiber Optic Profile/Downhole Steel Tube Cable. Source: Silixa

Figure 2. Fiber Optic Sampling Cable (2x10,000ft reels) w/testing box. Source: SLB/Geopsi

A testing box connected to the spool of the Fiber Optic Cable that allowed testing in the spool while RIH (Figure 2).

To the bottom of the FOC, an End Termination was installed to stop fluid ingress and allow pressure test (Figure 3). The End Termination was protected from mechanical damage during run in hole by tubing and Cross Collar Clamps.

Figure 3. Fiber Optic End Termination. Source: Silixa

Surface Cable

To connect the fiber safely on surface, a special fiber optic surface cable was trenched from the wellhead to the DTS Interrogator (Figure 4)

Figure 4. Surface Cable. Source: Silixa

Junction box

A NEMA 3R junction box was installed (Figure 5), where the surface cable and the downhole fiber get spliced and protected from the environment.

Figure 5. Junction Box. Source: SLB

Long Term DTS Data Acquisition

The interrogator is installed inside a NEMA3 enclosure, custom built by SLB (Figure 6) The enclosure contains:

-DTS box
-100-200VAC to 24 VDC power supply
-120/240VAC power switch
-UPS battery backup
-Fan
-Cellular modem

Figure 6. DTS Interrogator Enclosure. Source: SLB

The interrogator provided a full well profile every four minutes, as shown in Figure 7.

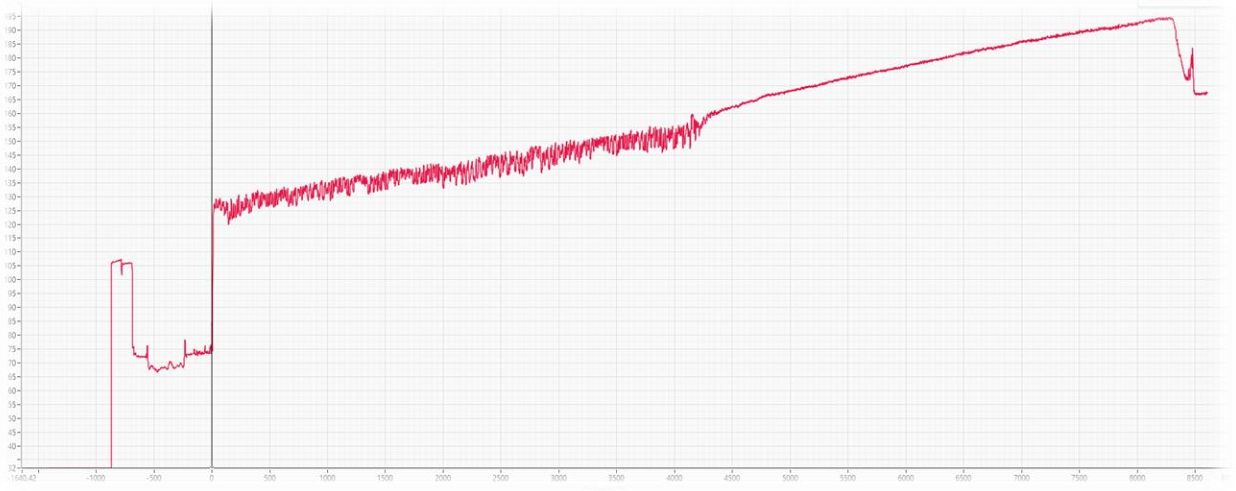

Figure 7. DTS Profile (Well 2). Source: SLB

The selected wells were located on the same pad in Martin County, Texas. The ESPs and FOC were deployed immediately following drill-out operations. Both ESPs were installed with identical downhole equipment and operated using the same variable speed drive (Table 1). The ESPs were ultimately removed after completing their full operational lifecycles and replaced with an alternative artificial lift method.

Well Name	Install Date	Pull Date	Run Days	Stage Type	Motor HP/V/A	VSD
Well 1	12/7/2024	12/12/2025	370	400UNB43H	416 / 3670 / 73	Smarten XE 513kVA
Well 2	12/5/2024	9/8/2025	277	400UNB43H	416 / 3670 / 73	Smarten XE 513kVA

Table 1. ESP Equipment details. Source: SLB

Observations collected over the operational months of both ESPs formed the basis for a series of tests, which are analyzed and discussed throughout this paper, in the following order:

Well 1:

1. Temperature profile above and below Bubble Point (Pb)
2. Heat dissipation from ESP to surface
3. Temperature profile during multiple shutdown events
4. Maximum temperature registered
5. Target speed to PID mode

Well 2:

6. Casing valve recirculation at surface
7. Temperature profile during slug operation

RESULTS

Well # 1

The lifetime performance trends for this well are presented below (Figure 8). The ESP intake pressure declined from 3,377 psi to 1,078 psi, while total fluid production decreased from 5,770 BPD to 778 BPD during operation with the first ESP, prior to conversion to an alternative artificial lift (AL) method.

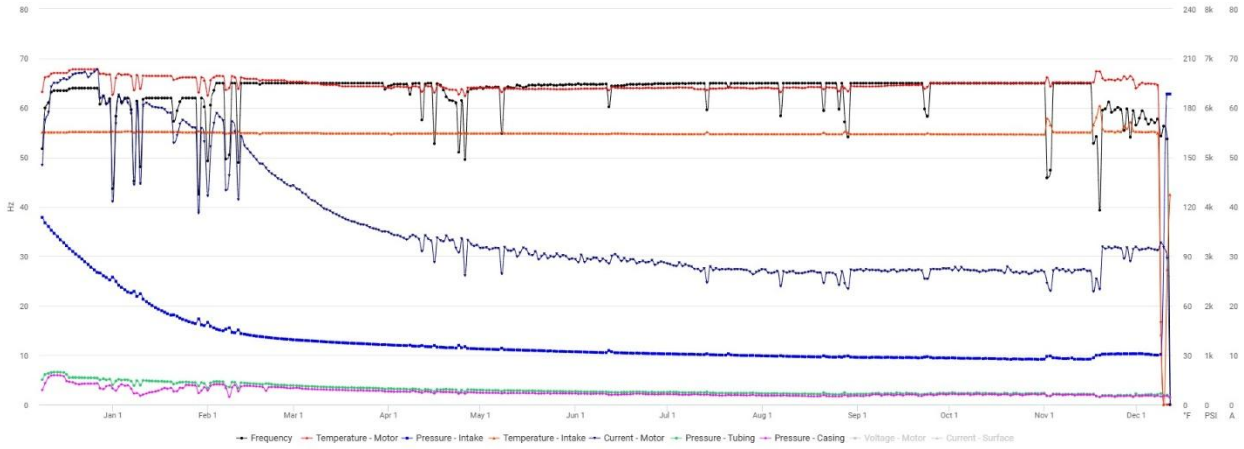

Figure 8. Well 1 Lifetime Trends. Source: SLB

1. Temperature profile above and below Bubble Point (Pb)

Objective - Test 1:
To determine the temperature profile during operation above and below the bubble point.

Result - Test 1:
The highest temperature observed in the ESP string during normal operation is localized above the pumps (Figure 9). Under these conditions, the temperature differential between the motor and the wellbore fluid is approximately 10°F. This differential increases to 25°F when compared to the temperature at the top of the pump (Table 2).

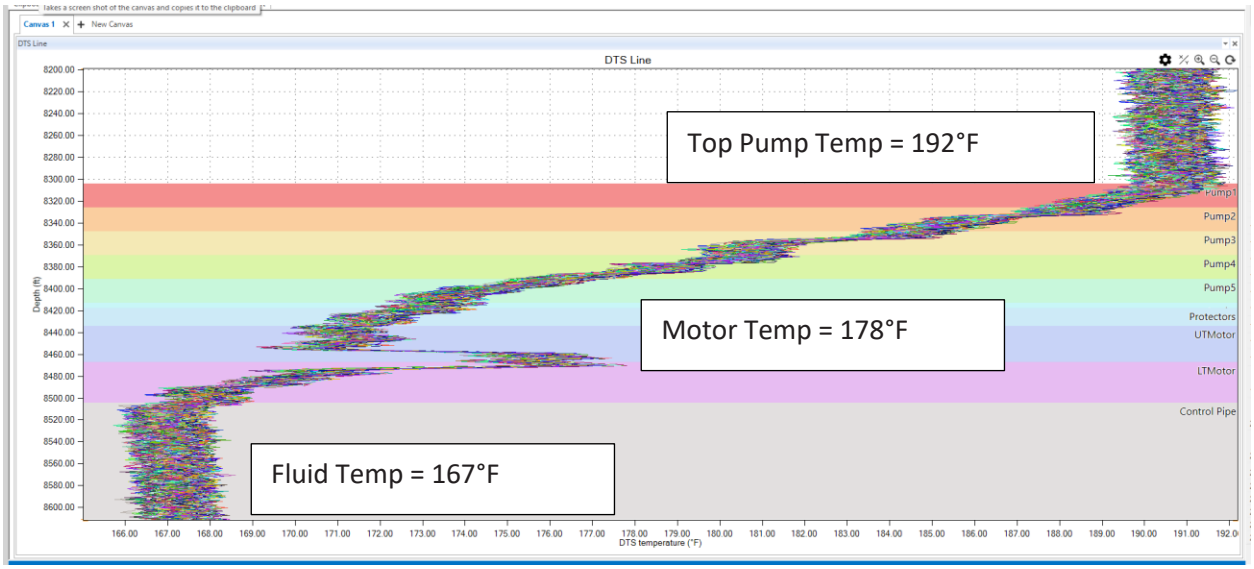

Figure 9. Temperature profile above Pb. Source: SLB

	Intake Temp (°F)	Motor Temp (°F)	Top Pump Temp (°F)
Sensor	165.90	198.50	
Fiber	167.00	177.72	191.92

Table 2. Temperature profile above Pb

When the well operates below the bubble point, performance becomes unstable due to the presence of free gas in the produced fluid (Figure 10). Under these conditions, and when there are no specific low- or no-flow events, the temperature differential between the wellbore fluid and both the motor and the pumps increases to approximately 31°F (Table 3).

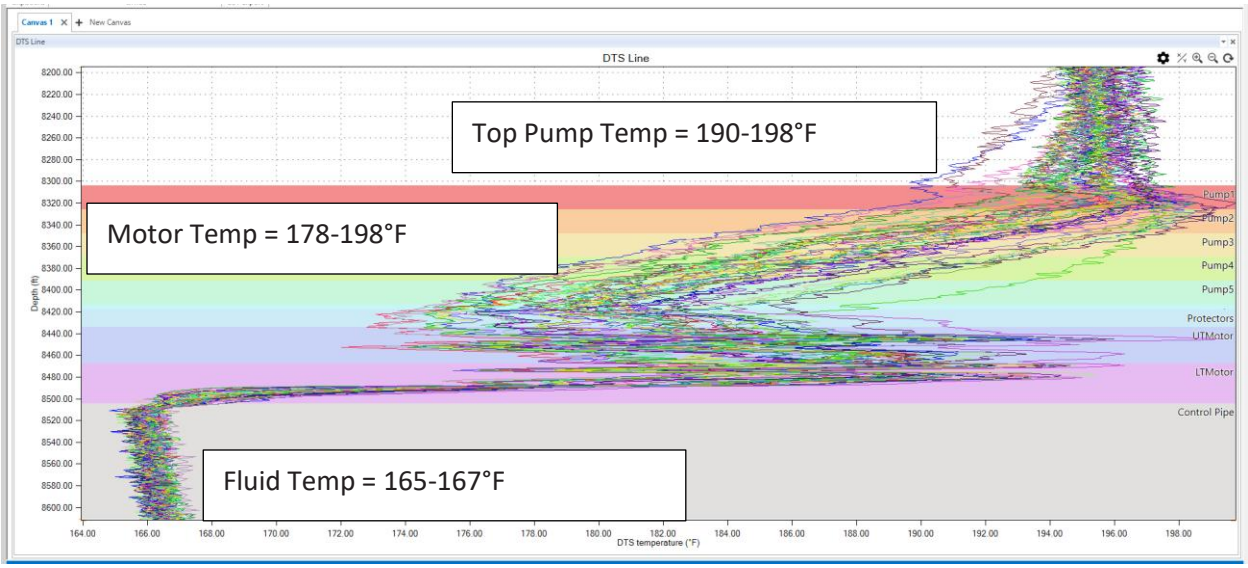

Figure 10. Temperature profile below Pb. Source: SLB

	Intake Temp (°F)	Motor Temp (°F)	Top Pump Temp (°F)
Sensor	165.3	194-195.8	
Fiber	165-167	178-198	190-198

Table 3. Temperature profile below Pb. Source: SLB

2. Heat dissipation from ESP to surface

Objective – Test 2:
To quantify the heat dissipation rate of this ESP and observe how the heat dissipates up the tubing and to surface.

Results – Test 2:
Figure 11 presents a screenshot captured during a power trip. At the bottom, the heat dissipation profile from the ESP to surface is observed. Approximately 30 minutes are required for the temperature at the top of the pump to equalize, during which heated fluid migrates upward until thermal equilibrium with the surrounding environment is achieved. During this 4-hour period before restarting the ESP, we can observe how much tubing space is equalized with the wellhead temperature of about 120°F.

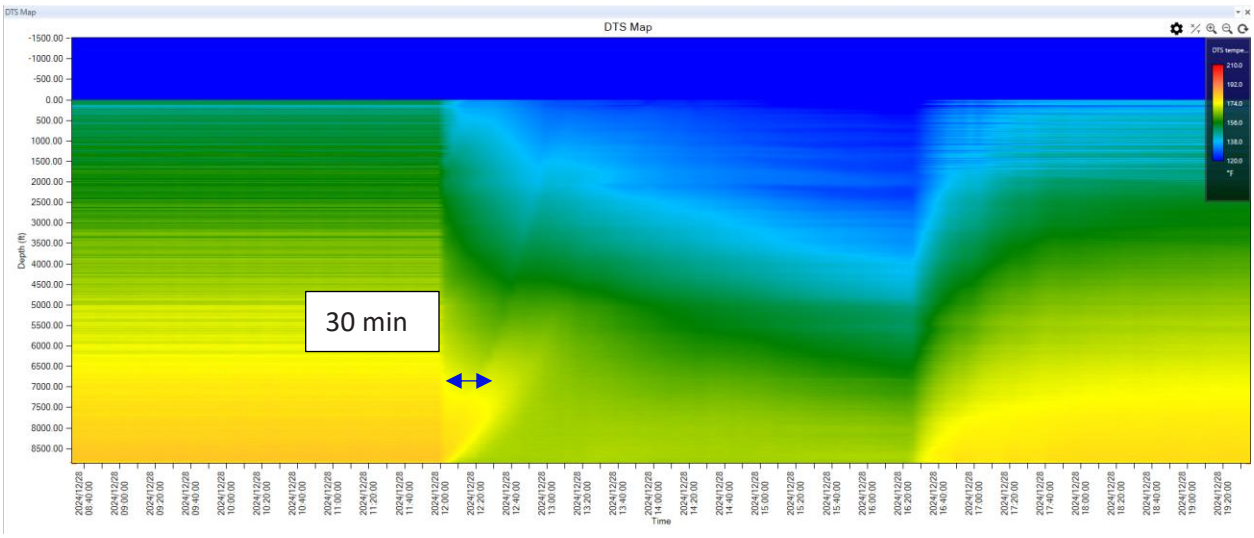

Figure 11. FOC Tubing Temp Profile. ESP heat dissipation. Source: SLB

3. Temperature profile during multiple shutdown events

Objective – Test 3:
During shutdown events, ESP sensors typically register an increase in temperature. The objective of this test is to evaluate the temperature response detected by the FOC along the ESP, the tubing profile during shutdown conditions, and to quantify the temperature differences observed when multiple shutdown events occur.

Results – Test 3:

Example 1. Speed Changes and Partial Plug
The events in Figure 12 represent a three-day period during which two winding-temperature shutdowns and one facility-related shutdown occurred. The VSD was operating in PID mode throughout these events.

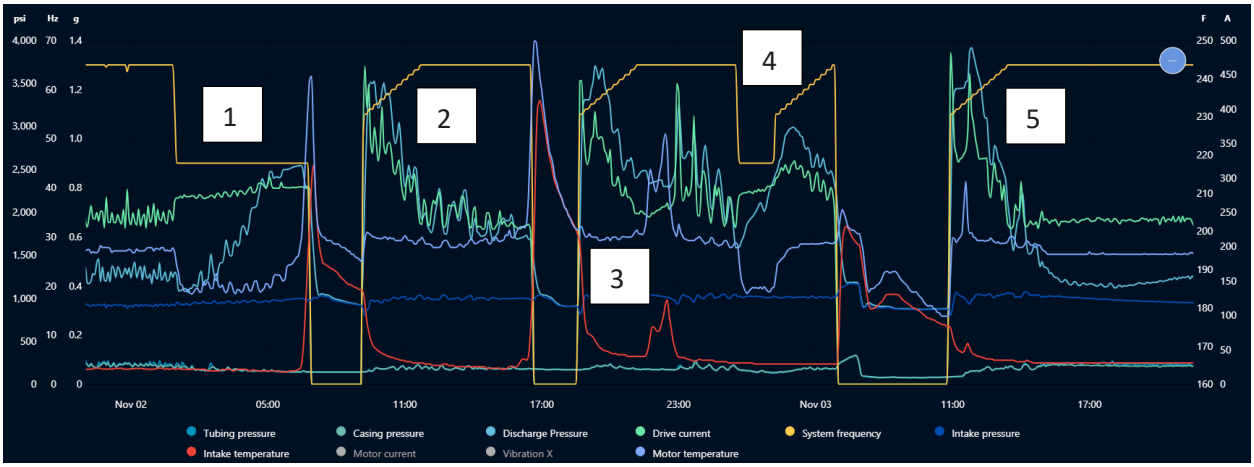

Figure 12. Multiple Shutdowns (numbered by event). Source: SLB

Event #1:
During Event #1, the VSD automatically reduced speed from 65 to 45 Hz in response to increased current during operation while running in PID mode. This behavior is believed to have resulted from a partial restriction between the pump and the wellhead, given the steady increase in current, discharge pressure and decrease in tubing pressure. Figure 13 between slowdown to 45Hz and the motor temp shut down shows a clear decrease in tubing temperature, likely associated with insufficient lift capacity.

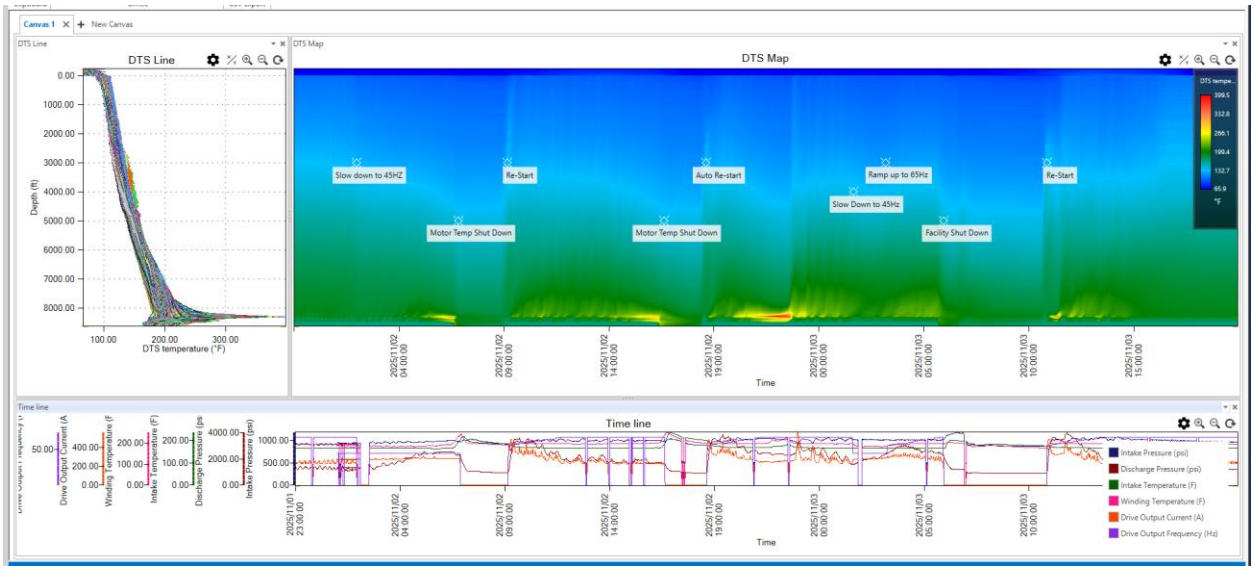

Figure 13. FOC Tubing Temp Profile after multiple shutdowns. Source: SLB

Immediately following the speed reduction, the motor temperature at the FOC increased slightly from 194°F to 206°F, temporarily exceeding the pump operating temperature of 197°F (Figure 14, left image). This thermal profile persisted for approximately two hours and fifteen minutes. Subsequently, pump temperature increased steadily for two hours and thirty-eight minutes until it reached 314°F, while motor temperature rose to 254°F (Figure 14, right image). The winding-temperature shutdown limit was set at 240°F at the sensor, resulting in a protective shutdown.

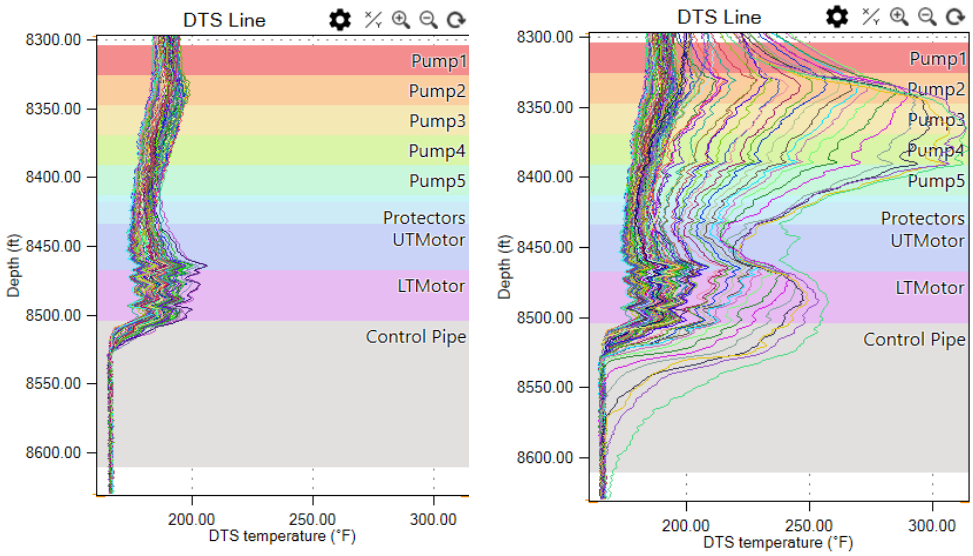

Figure 14. FOC ESP Temperature profile. Event #1. Left: Immediately after slowing down to 45Hz. Right: 2.5h after slowing down, before controller shutdown on winding temperature. Source: SLB

Event #2:
Approximately two hours later, the ESP was restarted remotely on target speed with an extended ramp to 65 Hz. Prior to this event, the normal operating current averaged 245 A. Upon restart, current peaked at 488 A before gradually declining to approximately 230 A, accompanied by a decrease in discharge pressure. The temperature profile at the ESP indicated that fluid was passing through the equipment but continuously losing energy. The controller shutdown when winding temperature again reached 240°F. At that point, the fiber optic cable recorded a pump temperature of 300°F and a motor temperature of 277°F.

The highest winding temperature registered by the downhole sensor (250°F) occurred immediately after this second shutdown. However, this temperature was only detected by the FOC as dissipated heat along the control pipe and did not exceed peak operating temperatures observed during operation.

Event #3:
The highest temperature registered by the fiber optic localized at the top pump was after the second shutdown, when the system was restarted before sufficient thermal dissipation had occurred. During Event #3, the ESP was restarted at 55 Hz and set on an extended ramp to 61 Hz. Initially, fluid starts to move up the tubing, however, between 20:10 and 22:00 (approximately two hours after restart), current and discharge pressure declined, tubing pressure decreased, and temperature increased. This behavior may be associated with the delayed production of a gas pocket in the lateral section of the well. This hypothesis will continue to be presented throughout this paper. During this event, the FOC registered pump temperature reached 300°F and motor temperature reached 290°F. After reaching peak temperature, approximately 43

minutes were required for the system to dissipate heat and return to normal operating conditions at 22:43 (Figure 15)

Event #4
After the restart in event #3, the ESP was left running in target speed. During Event #4, facility constraints required the ESP to be slowed down from 65 to 45 Hz on location. An immediate reduction in temperature was observed at the FOC, decreasing from a range of 210–230°F to a maximum of 197°F at the top of the pump. At the same time, current and discharge pressure stabilized, intake pressure increased immediately after slowing down, but continued depletion trend. The ESP stayed at 45 Hz for approximately 1.5 hours before speed was gradually increased. Upon reaching 65 Hz, the system shut down on permissive (facility).

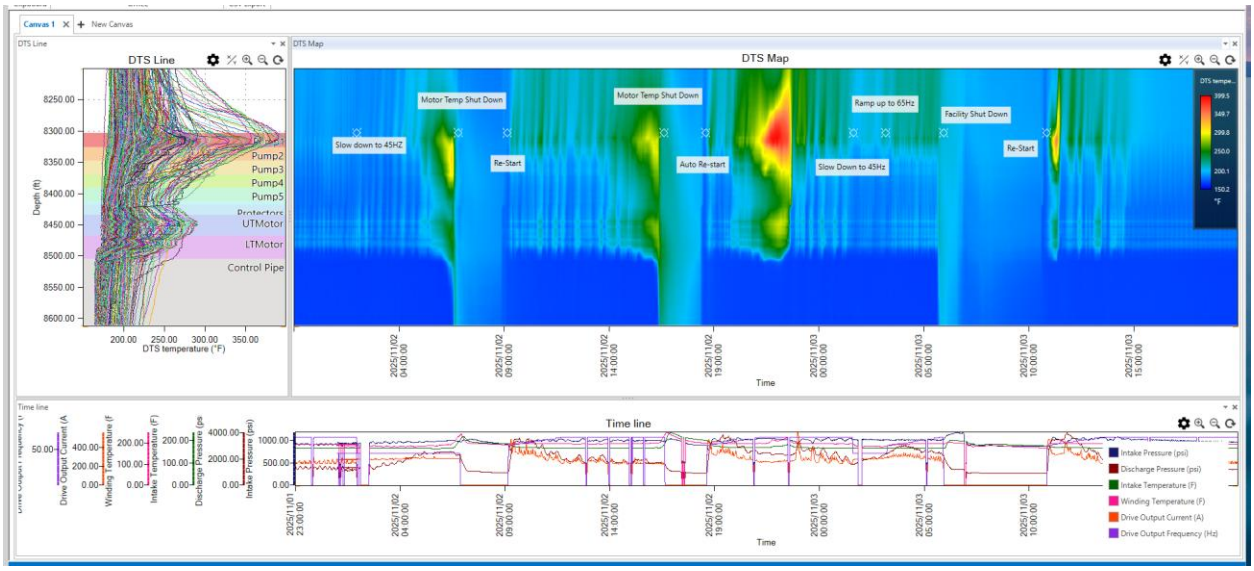

Figure 15. FOC ESP Temperature profile after multiple shutdowns. Source: SLB

Event #5:
Prior to Event #5, the ESP had been offline for approximately five hours. The unit restarted at 10:53 AM. Shortly after (11:04 AM), both pump and motor temperatures recorded by the FOC began increasing significantly, while current and discharge pressure measured by the sensor declined. This behavior indicates a low- or no-flow condition from a suspected gas pocket in the lateral.
The event lasted approximately 30 minutes (until 11:32 AM), after which the system regained lift and resumed normal operation.
The profile during normal operation at 65hz is represented in Figure 16. The maximum pump temperature at 200°F, motor temperature at 188°F, and intake temperature at 167.5°F.

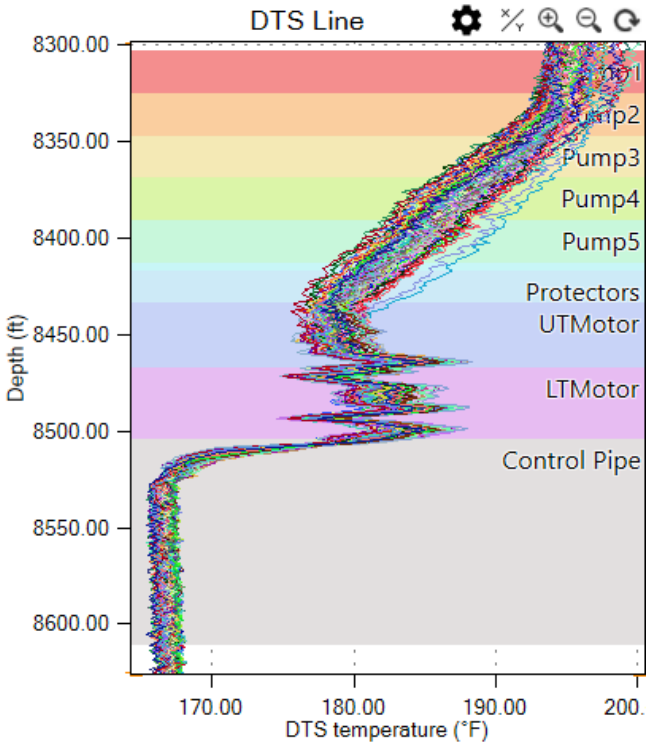

Figure 16. FOC ESP Temperature profile. Normal operation at 65 Hz. Source: SLB

Example 2. Consecutive PLC and UL Trips

The screenshot in Figure 17 represents a two-day event, where the ESP attempts to recover from a facility (PLC) shutdown, and fails to recover load on subsequent two restarts.

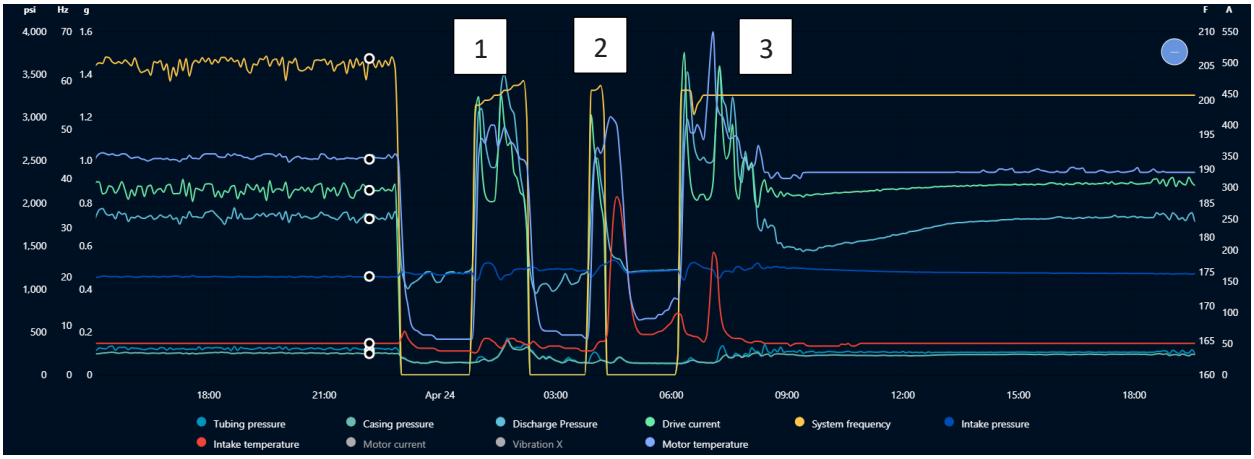

Figure 17. Trends consecutive PLC and UL Trips. Source: SLB

Event #1:

The ESP was restarted approximately two hours after a facility shutdown at 55 Hz (previously operating in PID mode at a maximum speed of 65 Hz). As demonstrated in

the previous example, the maximum temperature typically occurs several minutes after restart, when the produced fluid begins to lose energy (Figure 18 Event #3).
Trend data indicate that tubing pressure continued to build until 1:07 AM, 14 minutes after restart. A loss of energy consistent with a low- or no-flow condition was subsequently observed, exhibiting the characteristic indicators of gas interference. The fiber optic cable recorded an increase in pump temperature beginning at 1:09 AM, peaking at 237°F at 1:21 AM, and returning to baseline by 1:33 AM. The total duration of the thermal event was approximately 24 minutes. Tubing pressure began increasing again near 1:21 AM.
Following the restart, motor current steadily declined, and the controller ultimately shut down the ESP on underload 1 hour and 26 minutes after startup.

Event #2:
The subsequent restart was performed manually on location. The ESP started at 58 Hz and ramped to 59 Hz before tripping again on underload after 26 minutes.
Although energy loss was again observed during this restart attempt, the shorter event duration prevented pump temperature from exceeding 200°F. After shutdown, the downhole sensor recorded a maximum intake temperature of 186°F, which was read by the FOC as heat dissipation along the control pipe (Figure 19, Event #2).

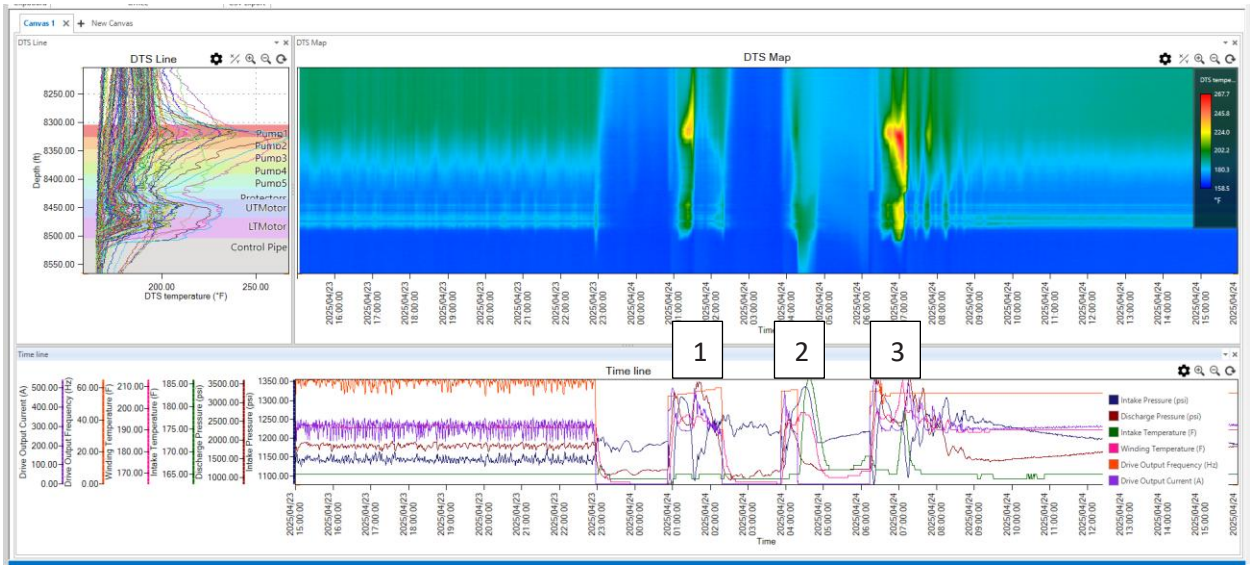

Figure 18. FOC ESP temperature profile after multiple shutdowns. Source: SLB

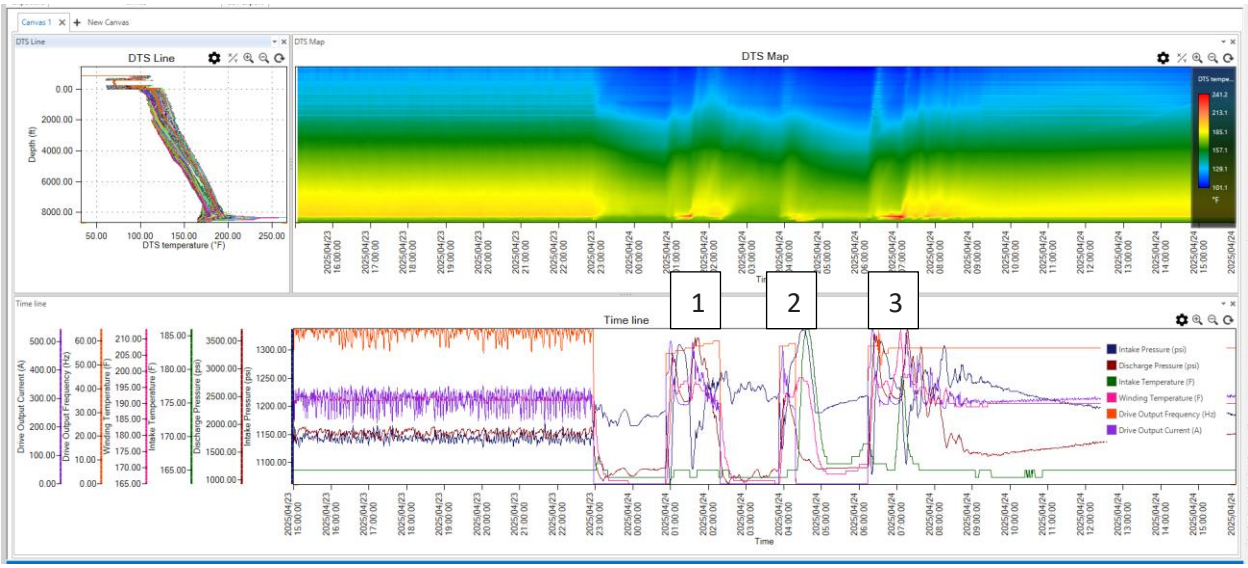

Figure 19. FOC Tubing Temperature profile after multiple shutdowns. Source: SLB

Event #3

The highest temperature recorded during this test sequence occurred during Event #3 (Figure 19). The ESP auto-restarted approximately two hours after the previous shutdown, initiating at 58 Hz at 6:14 AM.

This 28-minute low- or no-flow event increased pump temperature from 192°F to 267°F. The analysis of this event presented in Figure 20 correlates the FOC response when pump temperature started to increase, when it reached peak temperatures and when heat started to dissipate.

The sequence of surface and downhole responses is analyzed as follows:

- The VSD reported decreasing current beginning at 6:22 AM, while tubing pressure continued to build. Current increased again at 6:47 AM, briefly regained load, and then peaked again starting at 7:08 AM.
- Tubing pressure increased steadily for 18 minutes, reaching 272 psi, before declining to 130 psi at 6:32 AM. Pressure began rebuilding at 7:10 AM.
- The downhole sensor indicated that discharge pressure began decreasing at 6:29 AM and recovered at approximately 7:10 AM.
- Motor and intake temperatures began increasing at 6:52 AM and returned to baseline at approximately 7:24 AM.
- The FOC recorded an increase in pump temperature beginning at 6:33 AM, peaking at 7:02 AM to 267°F, and dissipating to normal temperature of 192°F by 7:12 AM.

This small analysis suggests that tubing pressure provides the closest correlation to the temperatures observed by the FOC temperature profile, followed by discharge pressure and load from current or the VSD. Therefore, these parameters are recommended as leading indicators of increases of temperature at the pumps. Other changes in readings at the downhole sensor such as motor temperature or intake pressure could also work

as indicators, but they should be considered as lagging indicators and therefore not the best indicator of thermal risk.

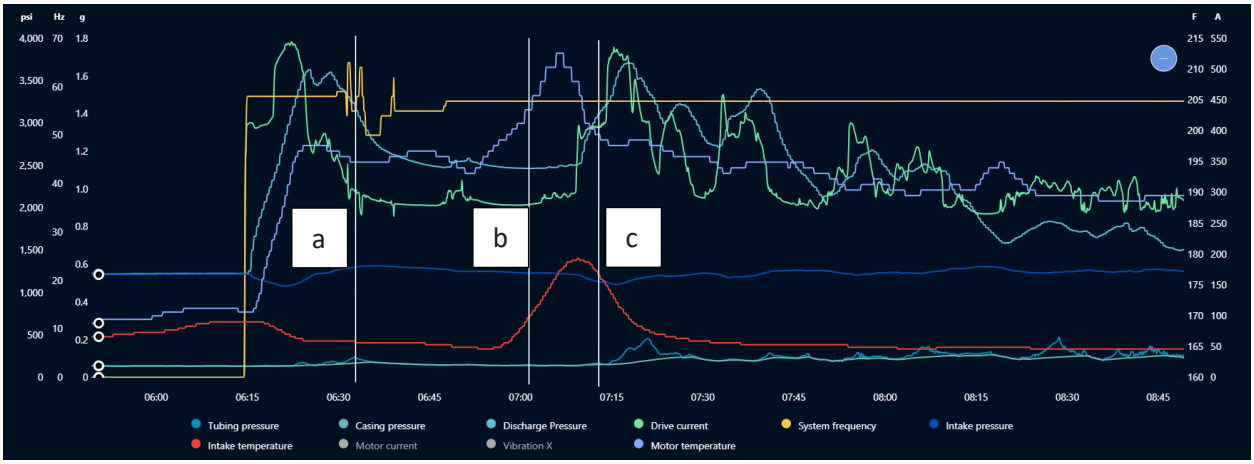

Figure 20. Trends Event #3. FOC a) Increase in pump temp, b) peak and c) dissipation. Source: SLB

After these events, the ESP continued operation at the max speed of 65 Hz. Maximum pump temperature at 192°F, motor temperature at 185°F, and intake temperature at 167.5°F (Figure 21)

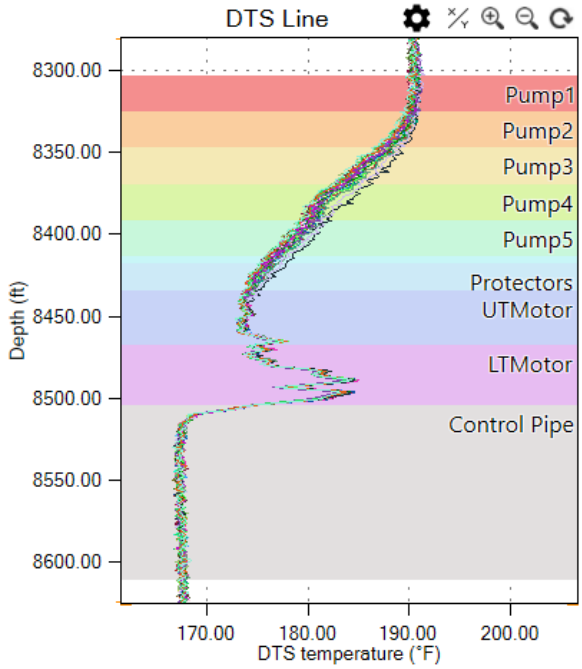

Figure 21. FOC Temperature profile normal operation for example 2. Source: SLB

4. Maximum Temperature Registered

Objective – Test 4:
To identify the highest temperature recorded by the fiber optic cable over the operational lifetime of the well and to identify the cause of this temperature event.

Results – Test 4:
The fiber optic cable recorded a maximum temperature of 400.7°F during an event on November 19, 2025, between 09:30 and 09:49. This event corresponded to the sixth restart in an abnormal operational sequence that began with a facility shutdown, followed by seven additional temperature-related shutdowns, until gas lock mode was activated to maintain load (Figure 22).

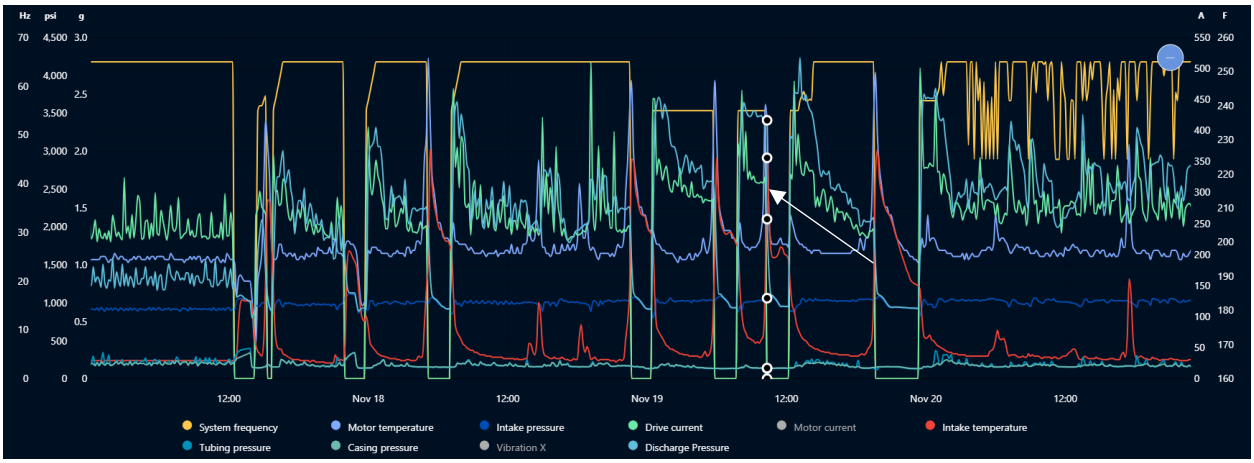

Figure 22. Trends, events corresponding to the maximum temperature event registered by FOC. Source: SLB

Unlike the cases presented above, these events represent confirmed motor temperature trips. During each event, tubing pressure increased only marginally above baseline, and the ESP tripped on motor temperature due to insufficient lift. The event associated with the highest pump temperature occurred within two hours of a prior motor temperature shutdown, during which the ESP had been restarted at a lower speed than normal operating conditions. This attempt lasted two hours and twenty minutes. During this period, tubing pressure dropped to baseline and remained at that level for approximately one hour prior to shut down, while discharge pressure remained higher than usual (Figures 23 and 24).

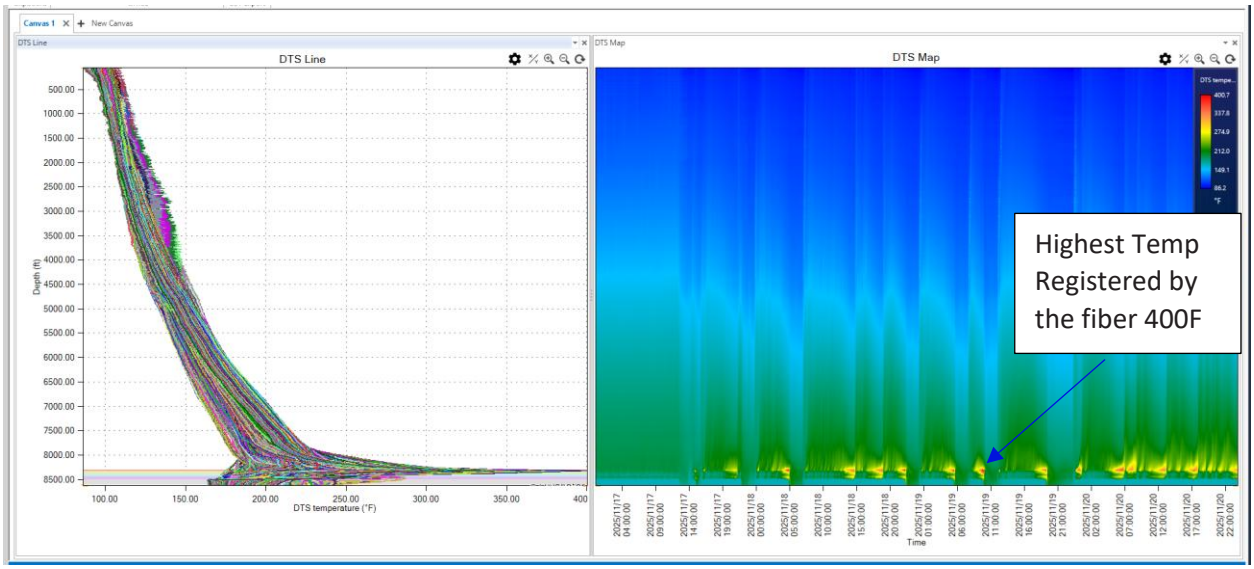

Figure 23. FOC Tubing temperature profile, power shutdown. Source: SLB

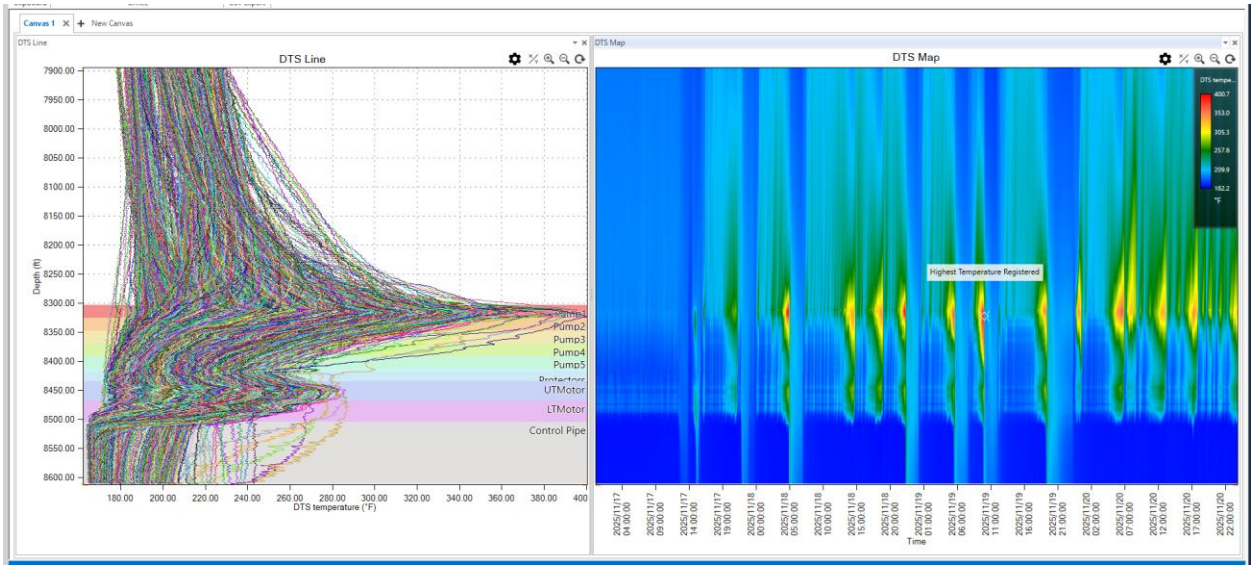

Figure 24. FOC ESP Temperature profile, power shutdown. Source: SLB

It is important to mention that the pump stages were found to be coated with scale after pulling the unit. This condition would have increased flow resistance, making it more difficult for the ESP to lift fluid to the surface prior to the proactive well intervention less than a month later.

This test reinforces the observation that the temperatures at the pump are highest during multiple shutdown and restart events and get exacerbated when the event is related to high winding temperature trips; with the FOC reporting a temperature differential of 120F between the top of the pumps and the motors. Following the shutdown, we observe pronounced heat dissipation signatures. This response shortens

the effective cooling period before restart, contributing to elevated pump temperatures on the next restart.

5. Target Speed to PID Mode

Objective – Test 5:
To analyze the temperature difference between operating in target speed and activating controller settings such as PID mode, to enable self-regulation of speed and stabilization of motor current during normal operation.

Results – Test 5:
Early adjustments to ESP parameters facilitate the work of the optimization engineer, allowing more efficient identification of appropriate control parameters. During this test, motor current variation was minimal, ranging from 33 A to 36 A, but there was an attempt to revert this trend to baseline by changing from target speed to PID mode, as observed on Figure 25.

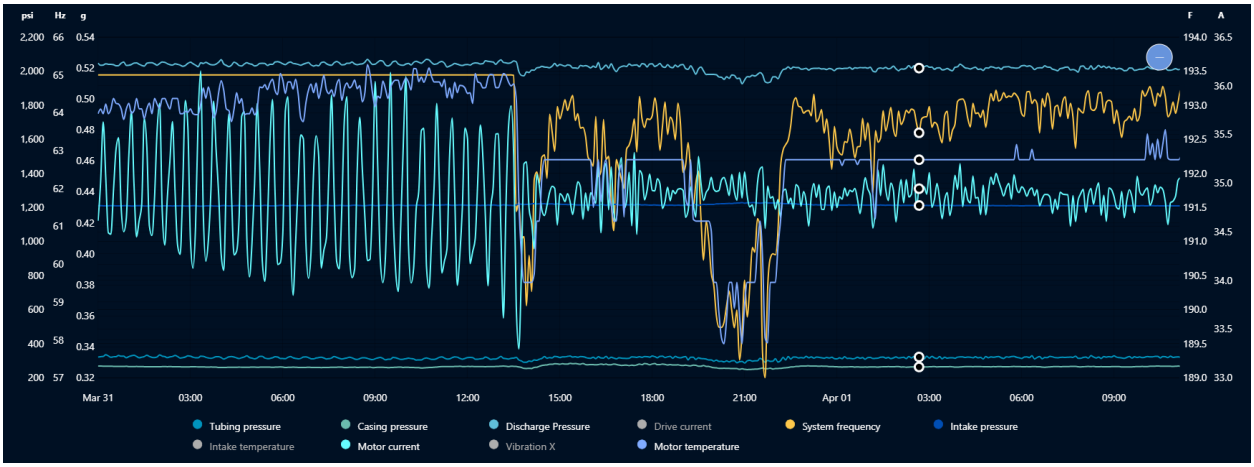

Figure 25. Trends. Target speed to PID. Source: SLB

As shown in Figure 26 (left), a current variation of approximately 3 A corresponded to a pump temperature change of 5°F and a motor temperature change of 7°F. With timely adjustments, motor current stabilized at 34 A, reducing temperature fluctuations to approximately 2°F for both the pumps and the motors (Figure 26, right).

Operating wells in the Permian Basin frequently involve managing slug flow conditions. Erratic performance is often observed when operating below the bubble point, and the magnitude of temperature increases at both the pump and motor is closely linked to the amplitude of current fluctuations (Figure 27).

This test shows the value of using the software technology on VSD controllers to take early corrective actions to help the ESP self-regulate and as a result, decrease the overall temperature of the string.

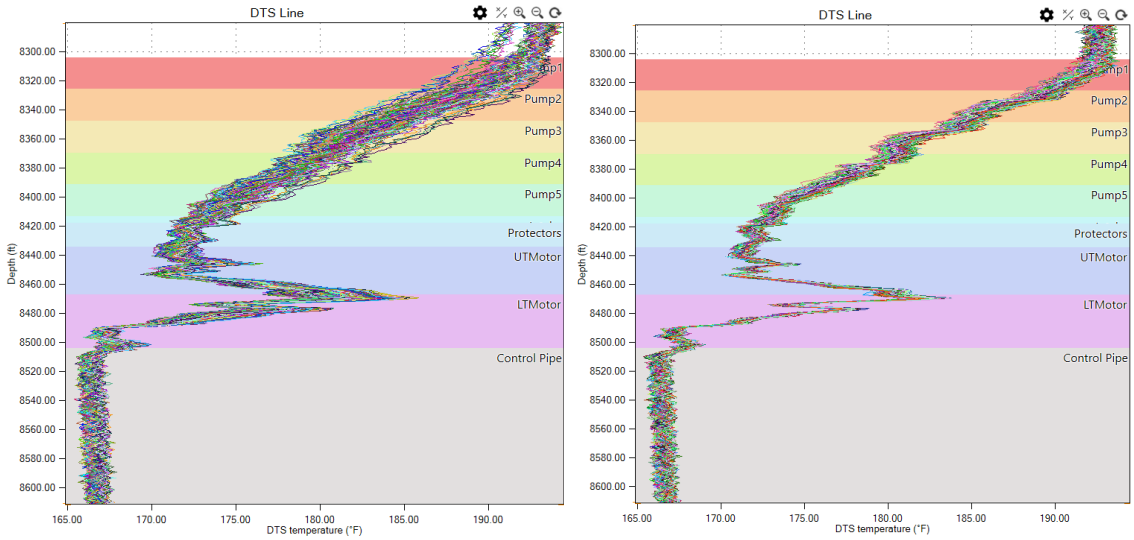

Figure 26. FOC ESP Temperature Profile. Comparison 3A swings (left), vs steady current (right). Source: SLB

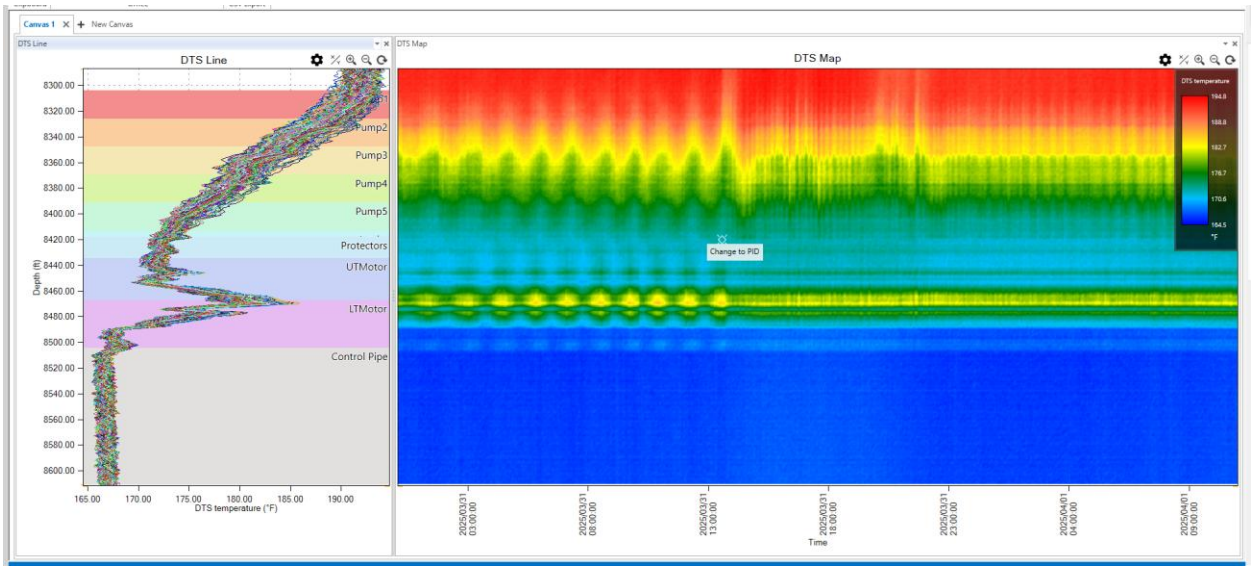

Figure 27. FOC ESP Temp Profile Target Speed to PID. Source: SLB

Well # 2

The lifetime performance trends for this well are presented below (Figure 28). The ESP intake pressure declined from 3,860 psi to 1,100 psi, while total fluid production decreased from 5,700 BPD to 675 BPD during operation with the first ESP, prior to conversion to an alternative artificial lift (AL) method. Figure 29 presents the normal operating temperature profile, showing the highest temperature above the top pump, reaching 200°F, and a maximum motor temperature of 187°F. Source: SLB

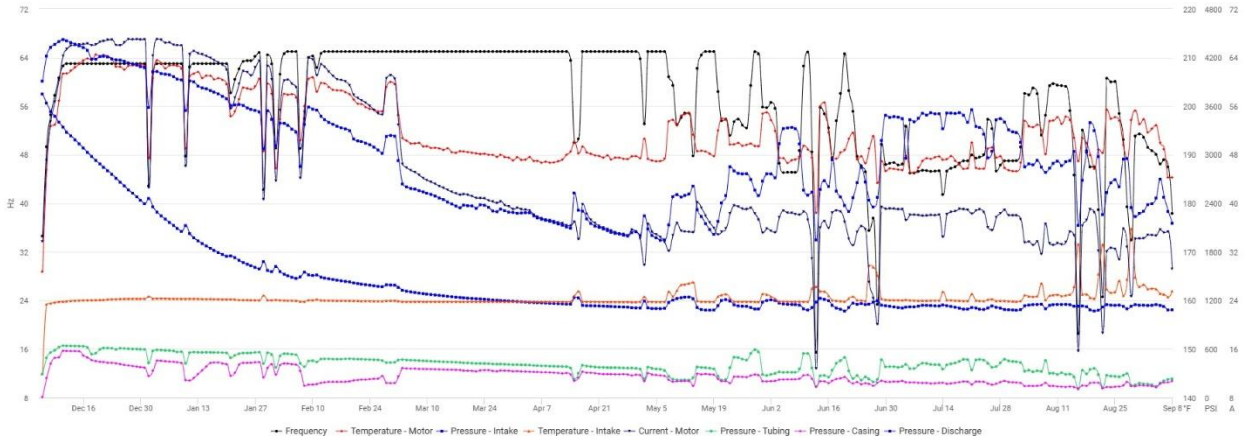

Figure 28. Well 2 Lifetime Trends. Source: SLB

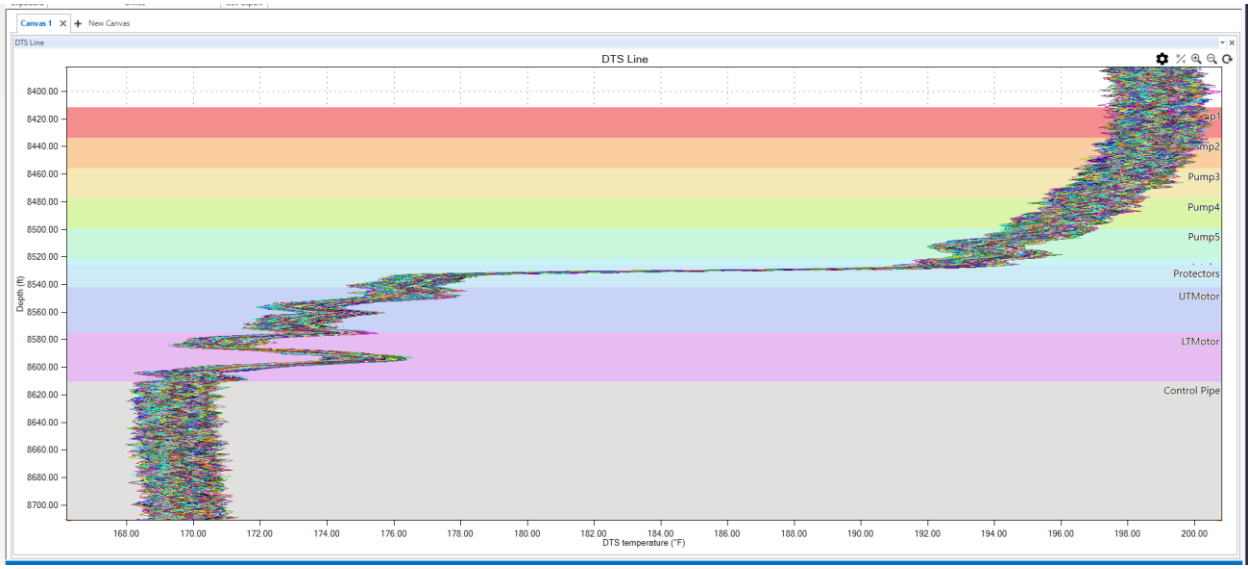

Figure 29. Well 2 Temperature Profile. Source: SLB

6. Casing valve recirculation at surface

Objective – Test 6:
To evaluate the effect of surface casing-valve recirculation on tubing temperature and ESP temperature behavior.

Results – Test 6:
Early in the life of Well #2, an operational change was observed following an event in which surface casing pressure increased. During this event, discharge pressure rose by approximately 200 psi above normal operating conditions, and a slight rise in motor operating temperature was observed, as measured at the downhole sensor (Figure 30).

Figure 30. Trends, casing valve recirculation. Source: SLB

Analysis of the fiber optic data revealed a distinct temperature pattern. Tubing temperature (Figure 31) increased during the event, which was subsequently identified as severe recirculation through a casing valve. Once the valve was fixed, the temperature profile returned to normal.

The most significant observation was the change in the ESP temperature profile (Figure 32). Under normal operation, a gradual temperature increase along the pump stages is typically observed, reflecting steady energy addition. However, during severe recirculation, the pumps did not exhibit this progressive temperature increase. Instead, the temperature at the top of the pump was nearly equal to that at the bottom of the pump, with temperatures returning to normal below the intake.
Motor temperature during these recirculation events remained close to baseline operating values, indicating that the primary thermal effect was localized at the pumps rather than the motor.

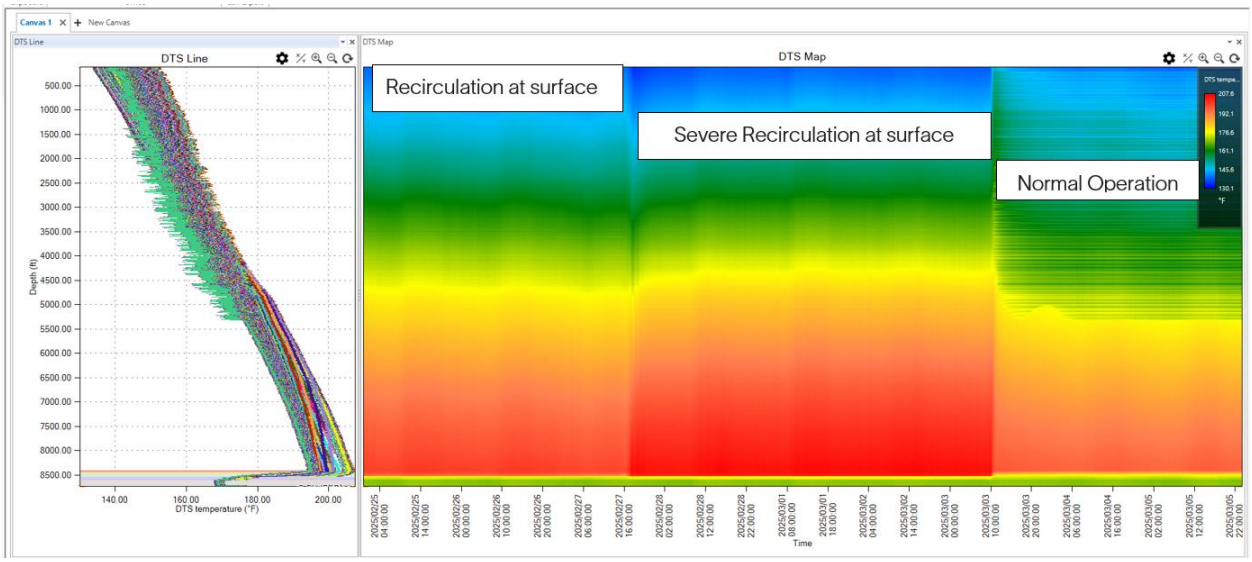

Figure 31. FOC Tubing Temp profile, casing valve recirculation. Source: SLB

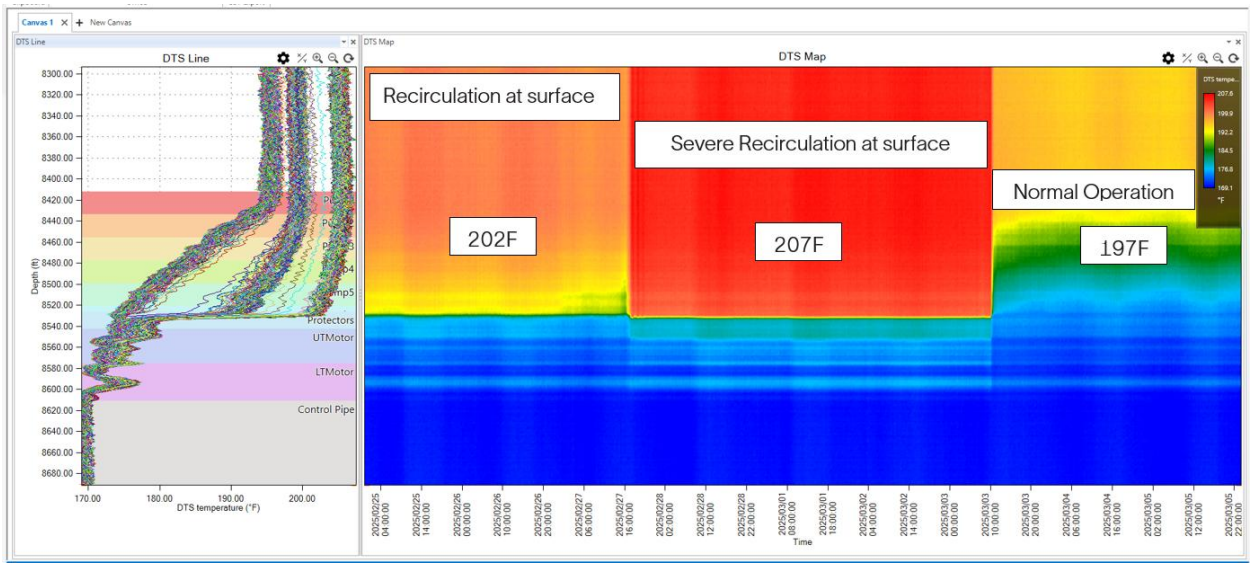

Figure 32. FOC ESP Temp, casing valve recirculation. Source: SLB

8. Temperature profile during slug operation

Objective – Test 8:
To evaluate the temperature profile under suspected slugging conditions, quantify the increase in ESP string temperature during these events, and determine the cooling rate of the string once fluid production resumes.

Result – Test 8:
Figure 33 illustrates events lasting between 20 and 35 minutes, followed by approximately 10 minutes of fluid production to surface. These events exhibit a pattern consistent with slugging operation. These events show pump temperature swings of up

to 100°F (Figures 34 and 35), depending on the time the low/no flow condition persists and cools back down very fast when fluid is loading again.

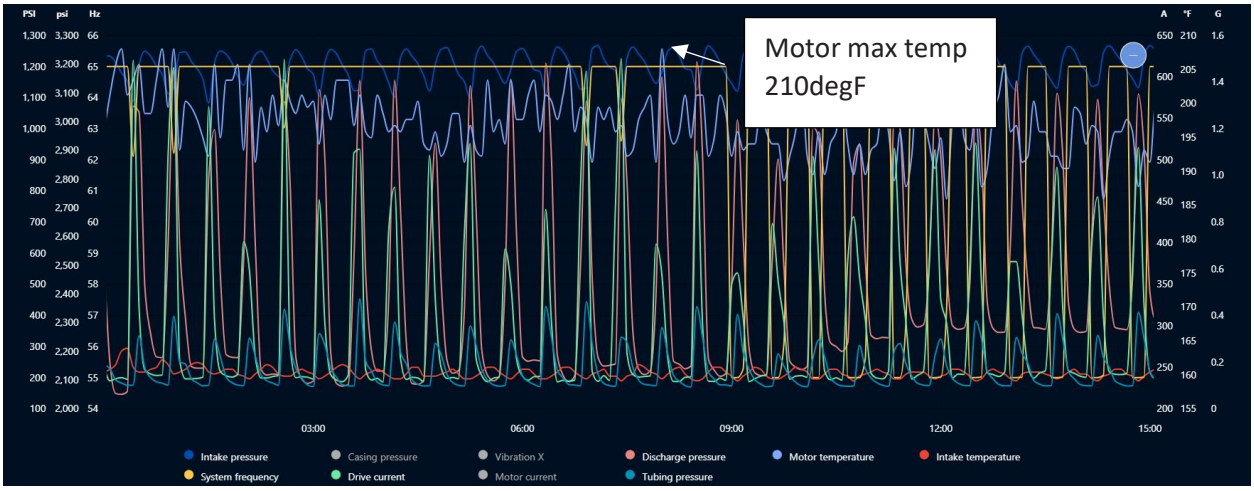

Figure 33. Trend Slug Operation. Source: SLB

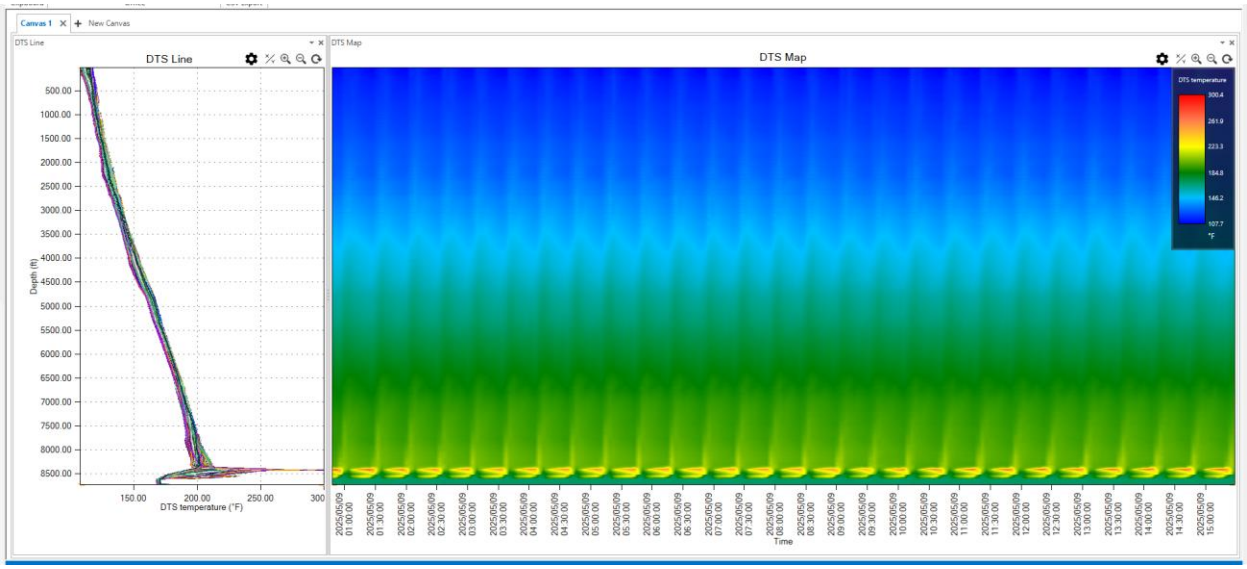

Figure 34. FOC Tubing temp profile, slug operation. Source: SLB

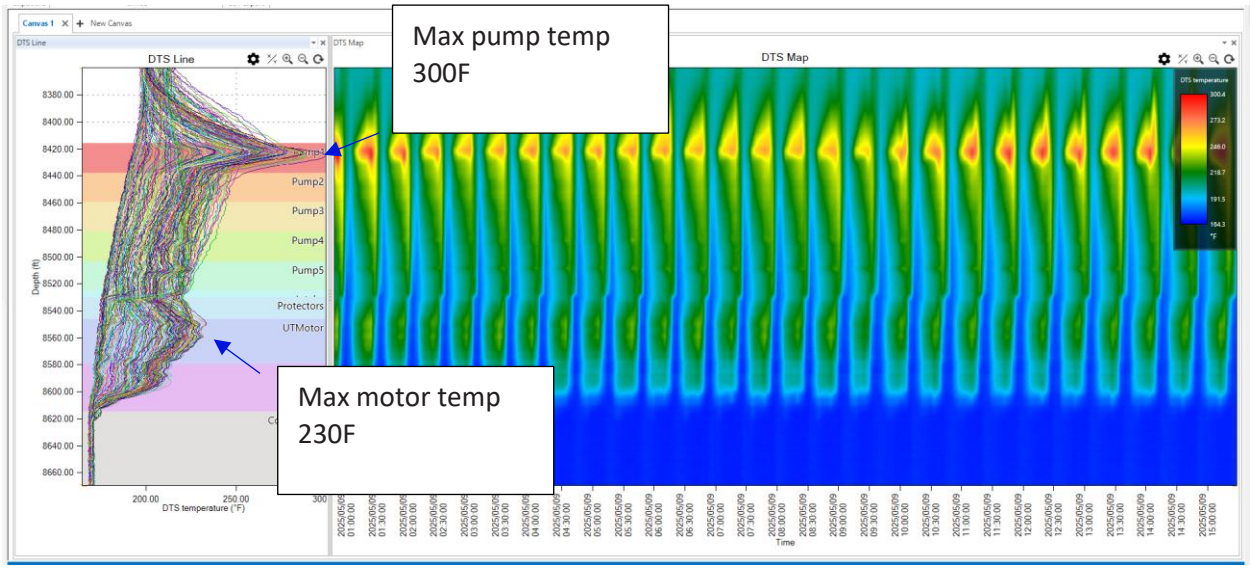

Figure 35. FOC ESP Temp profile, slug operation. Source: SLB

Figure 36 reconstructs the temperature profile at both the downhole sensor and the fiber optic cable in 4-minute increments. From the onset of the event to peak temperature, the temperature increases by 71°F over approximately 20 minutes, before declining to baseline conditions within 16 minutes.

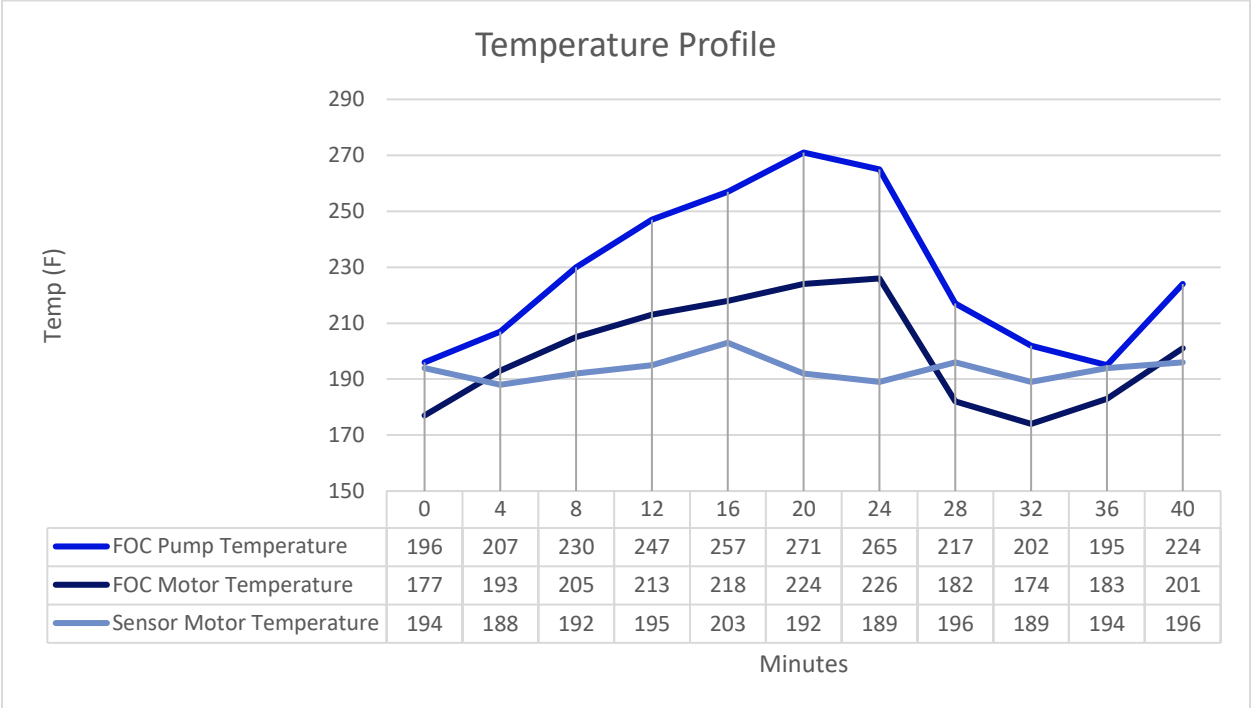

	0	4	8	12	16	20	24	28	32	36	40
FOC Pump Temperature	196	207	230	247	257	271	265	217	202	195	224
FOC Motor Temperature	177	193	205	213	218	224	226	182	174	183	201
Sensor Motor Temperature	194	188	192	195	203	192	189	196	189	194	196

Figure 36. Temperature Profile. 36 min event. Source: SLB

This test shows that the cooling rate is much faster than the temperature increase, but also the rate of the temperature increase at the pumps is significantly higher than winding temperature reported at the sensor, further signaling that motor temperature presents as a lagging indicator for temperature related events.

DISCUSSION

The temperature distribution along the ESP string under normal operating conditions follows a consistent pattern. The highest temperatures are observed above the pump stages, with temperature gradually declining toward the intake. A slight temperature increase is still evident at the head of each pump stage, reflecting incremental energy transfer to the fluid as it progresses through the system. This profile is indicative of stable hydraulic loading and continuous fluid movement.
In contrast, low- or no-flow conditions significantly alter this thermal behavior. During such events, the highest temperature is located at the top pump. The absence of adequate fluid movement results in rapid thermal accumulation at the pump discharge region.

Shutdown and restart events further highlight the sensitivity of the system to transient flow conditions. The highest temperatures during non-ESP related events (i.e. power or facility shutdowns) are not observed during or after the shutdown itself as normally reported by the downhole sensor, but rather after restart, particularly when fluid velocity to surface decreases and slugging occurs. These low-flow conditions create localized heating before steady production is reestablished. Based on repeated observations throughout this study, this behavior is believed to be associated with gas pockets accumulated along the lateral section, which are entrained and transported to the pump several minutes after restart. The delayed ingestion of these gas volumes temporarily disrupts hydraulic loading, contributing to reduced flow efficiency and rapid temperature increases at the pump.

ESP related shutdowns, such as winding temperature trips, result in the highest pump temperatures recorded by the fiber optic cable (FOC). While the FOC does not detect a significant increase in motor temperature during winding temperature–related shutdown events, it does capture a pronounced heat dissipation signature following the trip. This response shortens the effective cooling period before restart, contributing to elevated pump temperatures during subsequent operation. This effect is amplified during multiple shutdown cycles.

Electrical current fluctuations correlate strongly with thermal response: a 3 A motor current variation can result in approximately a 7°F change at the pumps, while a 32 A swing can produce temperature differentials of up to 100°F relative to wellbore fluid within 20 minutes. This demonstrates the rapid thermal sensitivity of the pump to load changes, and how important it is to utilize available VSD controller software in conjunction with optimization programs to act early and mitigate the severity of the thermal reaction during no flow or slug flow conditions.

Importantly, discharge pressure and motor current respond more quickly to low or no-flow events than motor temperature measurements. These parameters therefore serve as earlier indicators of developing thermal risk, whereas sensor winding temperature and other parameters such as pump intake pressure have a significant delayed response.

Overall, the findings demonstrate that pump temperature behavior is strongly governed by flow continuity, event duration, and control strategy. Managing transient low-flow events is therefore critical to minimizing thermal loading and extending ESP operational life.

CONCLUSION

An experimental R&D deployment of fiber-optic cable with continuous monitoring via a distributed temperature sensing (DTS) system was implemented in two unconventional wells in the Wolfcamp A formation, a reservoir characterized by gassy conditions below the bubble point. Observations collected over the course of a year on both ESP strings provided rare, high-resolution insight into downhole thermal behavior. While many findings confirm theories previously proposed by the industry regarding ESP performance in gassy wells, the data offers empirical validation that was previously lacking.

Key findings include:

1. Temperature distribution along the ESP string: under normal flow, the highest temperatures occur above the pumps, gradually decreasing toward the intake. Low- or no-flow events and slugging concentrate thermal accumulation at the top pump, highlighting the sensitivity of pump stages to transient flow regimes.
2. Impact of shutdown and restart cycles: peak temperatures are observed primarily during restart events due to transient slugging and delayed fluid movement. Multiple successive shutdowns amplify pump heating.
3. Larger current swings are directly correlated with rapid and significant temperature increases at the pump. Continuous surveillance to make proactive optimization changes using VSD controller software can make a big difference in electrical stress and consequent thermal reaction.
4. Electrical and hydraulic indicators of thermal risk: Discharge pressure and current respond more quickly than motor temperature, serving as early indicators of developing thermal stress.

Overall, the study provides rare empirical confirmation of industry hypotheses regarding ESP thermal behavior in gassy unconventional wells. These observations can inform more accurate operating envelope interpretations, refine cooling-related design assumptions, and enhance diagnostic capabilities using existing surveillance systems.

AKNOWLWDGEMENTS

This work was funded by SLB. The author acknowledges the company's investment in this project and its support in making this study possible. Special thanks are extended to the field operations team for their assistance in building the instrumentation, as well as for their support during installation and data acquisition. The author also thanks Diamondback Energy for their willingness to participate in this study and for granting permission to publish this work.

TABLES AND FIGURES